Diagn Interv Radiol 2024; DOI: 10.4274/dir.2024.242826

ABDOMINAL IMAGING

INVITED REVIEW

Tumor-like conditions that mimic liver tumors

Nir Stanietzky[1]
Ahmed Ebada Salem[2,3]
Khaled M. Elsayes[1]
Maryam Rezvani[2]
Kurt Fraivillig[1]
Usama Salem[1]
Sergio Klimkowski[1]
Mahmoud Diab[4]
Sagar Naik[1]
Ahmed Sobieh[5]
Christine O. Menias[6]
Akram M. Shaaban[2]

[1]The University of Texas MD Anderson Cancer Center, Department of Abdominal Radiology, Texas, USA

[2]The University of Utah, Department of Radiology, Utah, USA

[3]Alexandria University Faculty of Medicine, Department of Radiology, Alexandria, Egypt

[4]Suez Canal University Faculty of Medicine, Department of Radiology, Ismailia, Egypt

[5]University of Kentucky, Department of Radiology, Kentucky, USA

[6]Mayo Clinic, Department of Radiology, Arizona, USA

Corresponding author: Khaled M. Elsayes

E-mail: kmelsayes@mdanderson.org

Received 25 April 2024; revision requested 12 May 2024; accepted 05 June 2024.

Epub: 14.06.2024

Publication date:

DOI: 10.4274/dir.2024.242826

ABSTRACT

Non-neoplastic tumor-like conditions of the liver can appear similar to hepatic neoplasms. In many cases, a biopsy is required to confirm the pathology. However, several tumor-like conditions can be correctly diagnosed or suggested prospectively, thus saving patients from unnecessary anxiety and expense. In this image-focused review, we present the ultrasound, computed tomography, magnetic resonance imaging, and positron emission tomography scan features of eight such entities. Clues that indicate the correct pathology are discussed, and the usual clinical setting is described. Many of these lesions are treated differently from true neoplasms, and the current treatment plan is discussed in many of the cases presented. After reviewing this article, the reader will have a better understanding of these lesions and the situations in which they should be included in the differential diagnosis.

KEYWORDS

Benign hepatic lesion, hepatic amyloidosis, hepatic extramedullary hematopoiesis, hepatic pseudotumor, hepatic sarcoidosis, hepatic tumor mimics, hepatic tumor-like conditions, hepatobiliary tuberculomas, liver imaging, mesenchymal hamartoma, myofibroblastoma, peliosis hepatis

Differentiating hepatic tumors from tumor-like conditions can be challenging because the imaging features may overlap. An understanding of several of the more common tumor-like lesions that can be misdiagnosed as tumors is vital so that the correct pathology can be included in the differential diagnosis. In this article, we describe the clinical and imaging features of some of the more common tumor-like conditions to assist radiologists in determining the correct diagnosis.

Mesenchymal hamartoma

Mesenchymal hamartomas of the liver (MHL) represent only 5% of pediatric tumors. However, after infantile hemangiomas, they are the second most common benign liver tumors in children younger than 5 years. The lesions normally present as painless abdominal distention in a patient with a normal or slightly elevated alpha fetoprotein level.[1] In some cases, the alpha fetoprotein level is substantially elevated, leading to diagnostic confusion. The tumors can be very large (up to 20–30 cm).[1] Mesenchymal hamartomas are associated with Beckwith–Wiedemann syndrome and multiple congenital fetal anomalies.[2] Most cases (75%) arise from the right hepatic lobe, and up to 20% of tumors are pedunculated.[1]

On imaging, an MHL appears as a large, well-demarcated, multilocular cystic mass with septal and/or stromal enhancement (Figure 1). On magnetic resonance imaging (MRI), the cystic components demonstrate high signal intensity on T2-weighted images and variable signal intensity on T1-weighted images as a result of hemorrhagic or proteinaceous debris (Figure 2). The solid and stromal components are mildly enhanced by the administration of intravenous gadolinium.[3]

Histologically, MHLs are composed of hepatocytes, haphazardly arranged bland spindle cells, and benign bile ducts in a collagenous stroma.[1,4] They have no malignant features and are usually cured through surgical resection. On rare occasions, MHLs have been theorized to progress to embryonal sarcoma, as the two entities have similar molecular alterations in chro-

You may cite this article as: Stanietzky N, Salem AE, Elsayes KM, et al. Tumor-like conditions that mimic liver tumors. *Diagn Interv Radiol.* 14 June 2024 DOI: 10.4274/dir.2024.242826 [Epub Ahead of Print].

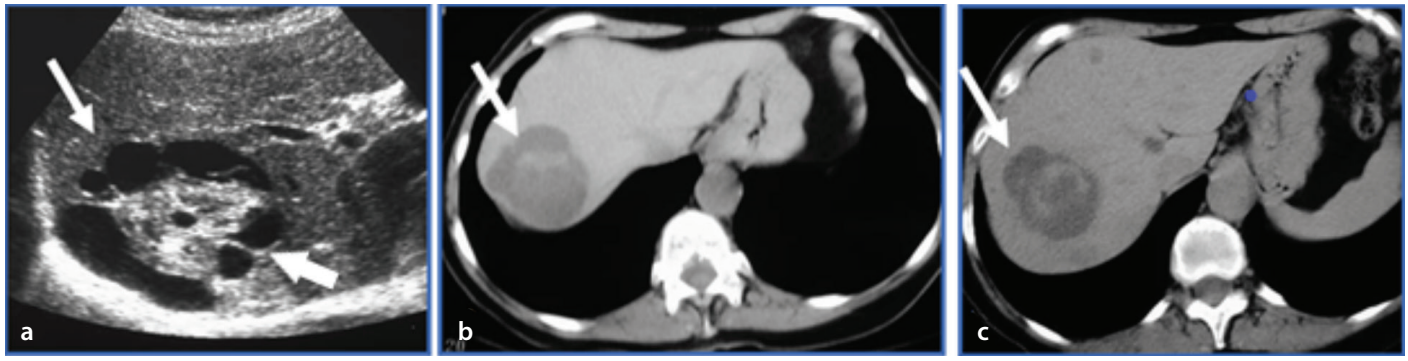

Figure 1. Grayscale ultrasound scan **(a)** showing a complex cystic mass with a solid component (white arrow). Non-enhanced computed tomography images **(b, c)** showing a mass in the right hepatic lobe (white arrows). The mass was predominantly cystic and had a central solid component. A mesenchymal hamartoma was identified through pathology.

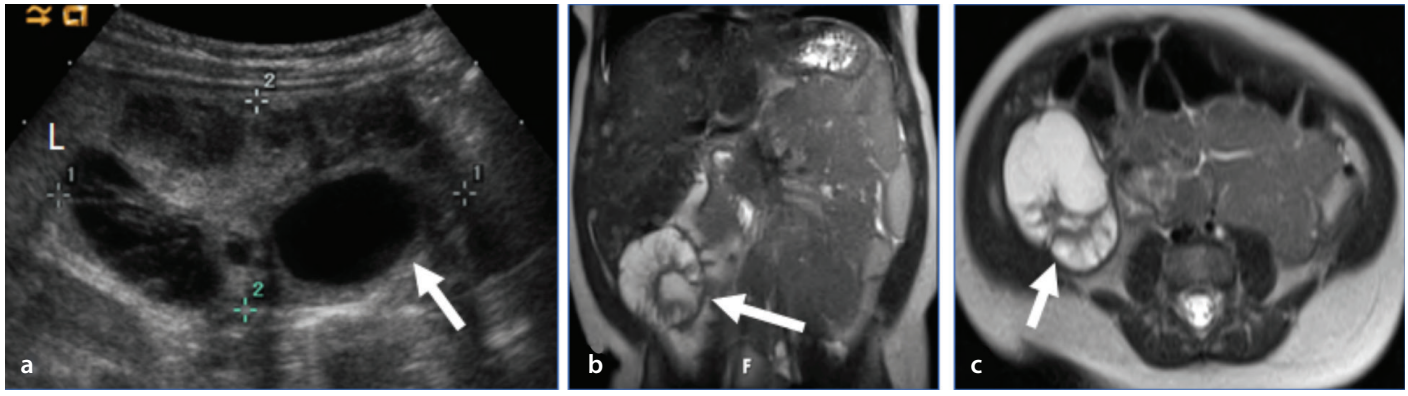

Figure 2. Grayscale ultrasound scan **(a)** showing a mixed solid and cystic mesenchymal hamartoma (white arrow) arising from the inferior aspect of the liver (L). Coronal **(b)** and axial **(c)** T2-weighted images showing a complex cystic mass with internal septations (white arrows).

mosome 19.[1] Additionally, there have been case reports of benign bile duct-like structures in the periphery of embryonal sarcomas with a similar histologic configuration to MHL, raising the possibility that the MHL was the precursor lesion.[1] Therefore, complete surgical excision is crucial.[2] Rarely, symptomatic unresectable disease has necessitated liver transplantation.[2]

Myofibroblastoma

Myofibroblastomas (inflammatory pseudotumors), which represent less than 1% of liver tumors, are a heterogenous group of masses that form benign tumors composed of inflammatory cells and fibrous stroma. These tumors may be very slightly more prevalent in men. Patients are diagnosed at an average age of 50 years, and there is no association with cirrhosis. The etiology of myofibroblastomas is unknown; however, it has been hypothesized that they result from hepatic infection, cholangitis, or a vascular injury.[4,5] In most cases, the infectious agent is not identified. Some of these tumors occur in patients with immunoglobulin G4 sclerosing disease, and these patients may have a history of autoimmune pancreatitis or sclerosing cholangitis.[2,5] Patients may present with fever, abdominal pain, and weight loss. Most tumors are 2–5 cm in diameter when detected, but some patients have presented with tumors greater than 20 cm.[5] Patients may have elevated erythrocyte sedimentation rates, neutrophil counts, and C-reactive protein levels.[5] The pathologic features can overlap with other disease entities, and a subset requires next generation sequencing to aid in diagnosis.[2]

On ultrasound, myofibroblastomas present as well-circumscribed heterogeneous masses with solid and cystic components. On computed tomography (CT), they are commonly hypoattenuating compared with the liver on unenhanced images, and they usually demonstrate peripheral or septal enhancement on delayed images. At least part of the lesion may demonstrate delayed enhancement, presumed to be related to abundant fibrous tissue (Figure 3). On MRI, they are hypointense in T1-weighted images and isointense or hyperintense on T2-weighted images, with a similar postcontrast enhancement pattern to that seen on CT (Figure 4). Typically, no associated desmoplastic reaction occurs. The differential diagnosis includes cholangiocarcinoma, which can also demonstrate delayed enhancement, abscess, metastasis, and hepatocellular carcinoma.[6]

Myofibroblastomas are often treated conservatively because they may resolve spontaneously or respond to antibiotic therapy or steroid therapy. Although surgical resection is curative, it is generally reserved for cases in which no biopsy was performed or in which the diagnosis remained unclear after biopsy. Surgery may also be performed in cases in which the lesion does not respond to conventional therapy.

Main points

- Non-neoplastic lesions of the liver can appear similar to hepatic tumors. Although pathologic evidence is often necessary for a definitive diagnosis, including these entities in the differential diagnosis can aid the clinician with the diagnostic workup.
- Multiple clinical clues might suggest that a liver lesion is benign. Although these may not be definitive, key factors include normal tumor markers, a history of infection, and a history of a systemic disease known to involve the liver.

Extramedullary hematopoiesis

Extramedullary hematopoiesis (EMH) refers to the production of blood cells outside

the bone marrow, a phenomenon observed in patients with defective marrow synthesis (e.g., chronic myelofibrosis) or with conditions associated with peripheral red blood cell destruction (such as hemoglobinopathies and hemolytic anemias).[7] The liver and spleen are the most common sites for EMH. Organ enlargement, particularly hepatomegaly, is more frequently observed than discrete lesions. When discrete lesions do occur, they may present as single or multiple focal masses or as infiltrative periportal or peribiliary soft tissue lesions.[8,9]

On ultrasound, lesions associated with EMH can appear hypoechoic or hyperechoic and typically present as heterogeneously attenuated nodules.[10,11] CT generally reveals hypodense lesions with variable attenuation and may show no, mild, or heterogeneous enhancement (Figure 5).[10,12,13] In rare cases, lesions may exhibit fat density without enhancement.[14]

On MRI, EMH lesions have variable signal characteristics, depending on whether the lesion is functional (actively hematopoietic) or inactive. Active lesions typically exhibit intermediate T1 and high T2 signal intensities with mild to moderate enhancement (Figure 6). By contrast, inactive lesions, which are predominantly composed of fibrous tissue, indicate low T1 and T2 signal intensity with minimal or no enhancement.[12,15] Macroscopic fat, which can occur in inactive lesions, produces a signal intensity that detects fat in all sequences. In patients with transfusion-related hemochromatosis, decreased background hepatic signal intensity is seen on sequences most sensitive to magnetic susceptibility.[15] Despite these imaging findings, a definitive diagnosis usually requires pathologic evaluation, which often reveals erythroid or myeloid precursors along with fatty or fibrous tissue.[16]

Epstein–Barr virus-associated smooth muscle tumor

Epstein–Barr virus (EBV)-associated smooth muscle tumors are rare slow-growing mesenchymal tumors that primarily affect immunocompromised patients. The incidence is highest among individuals who are HIV positive, followed by patients with drug-induced immunosuppression after organ transplantation, and, less commonly, patients with congenital immunodeficiency disorders.[17-20]

These tumors impact both adult and pediatric patients and are slightly more prevalent among women.[21] Abdominal pain is frequently reported as the main presenting symptom.[17,21]

In patients with AIDS, multicentric involvement is common, either occurring simultaneously or sequentially.[22] Molecular analyses of such multicentric presentations have revealed distinct clonal origins for the lesions at each site, suggesting that these lesions represent multiple primary tumors rather than metastases.[20,23-25] The tumors can affect various organs, including the central nervous system, spleen, lungs, gastrointestinal tract, larynx, pharynx, skin, adrenal glands, and eyes. The liver is the most commonly involved organ in immunosuppressed

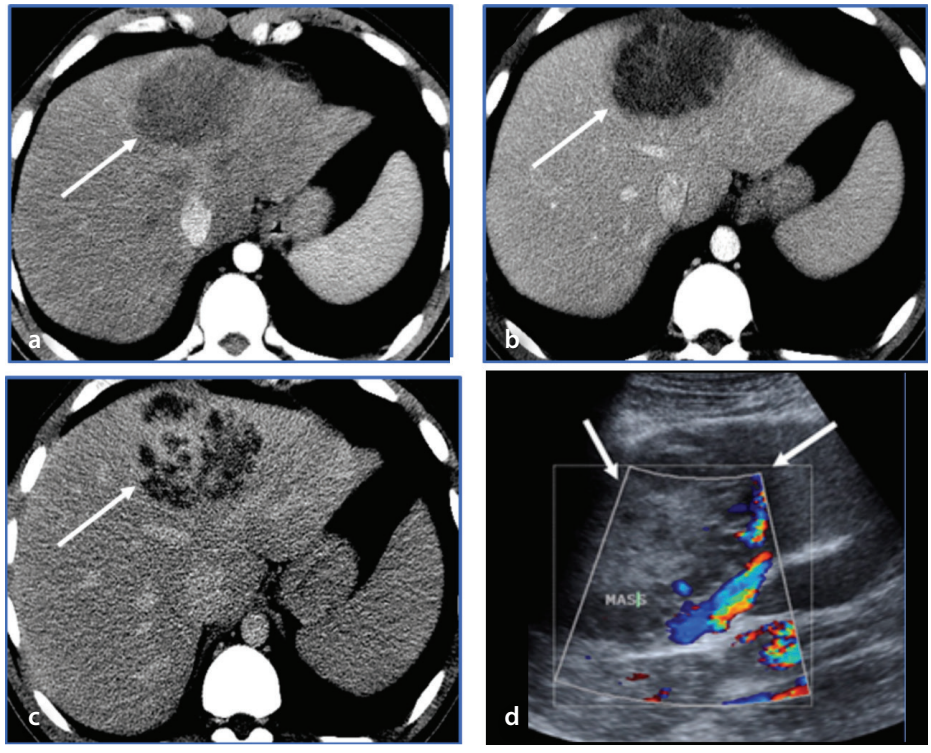

Figure 3. Axial contrast-enhanced computed tomography scans of a myofibroblastoma taken during the arterial **(a)**, portal venous **(b)**, and delayed **(c)** phases with a mass in the left hepatic lobe (white arrows), demonstrating poor enhancement during the arterial and portal phases and heterogeneous internal delayed enhancement during the delayed phase. Color Doppler ultrasound images **(d)** showing a multilobulated mass with an echogenic center, hypoechoic periphery, and minimal internal blood flow.

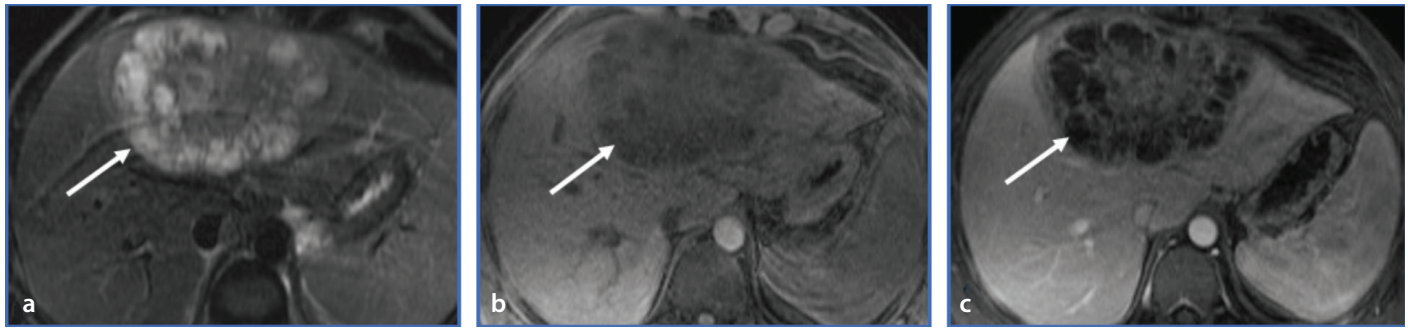

Figure 4. Additional case of a biopsy-verified myofibroblastoma. Axial T2-weighted image **(a)**, pre-contrast T1-weighted image **(b)**, and post-gadolinium T1-weighted image with fat suppression **(c)** revealing a multiloculated solid and cystic mass (white arrows) with numerous small T2-bright peripheral components and a more solid central portion that is mildly hyperintense on the T2-weighted image and mildly hypointense on the T1-weighted images. With contrast administration, septal enhancement and progressive delayed enhancement of the central component of the mass were identified.

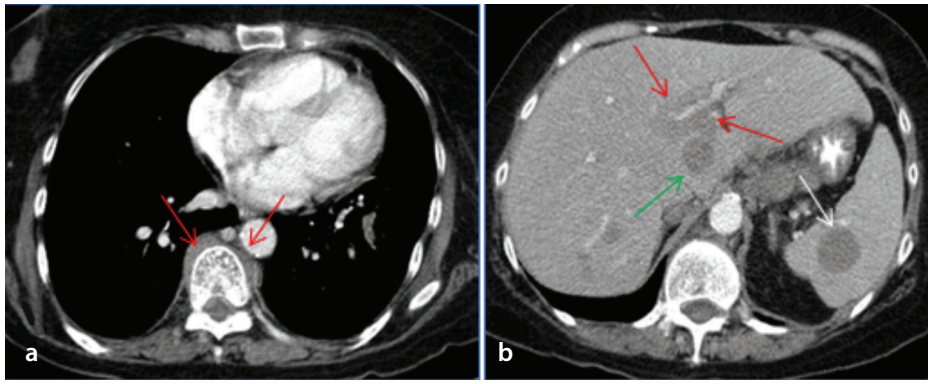

Figure 5. Contrast-enhanced computed tomography (CECT) images revealing extramedullary hematopoiesis in a 61-year-old woman with myelodysplastic syndrome. Axial CECT image **(a)** at the level of the lower chest showing paravertebral masses (red arrows). Axial CECT image **(b)** through the upper abdomen showing hepatic (green arrow) and splenic (white arrow) rounded hypoattenuating masses and periportal poorly enhancing tissue (red arrows).

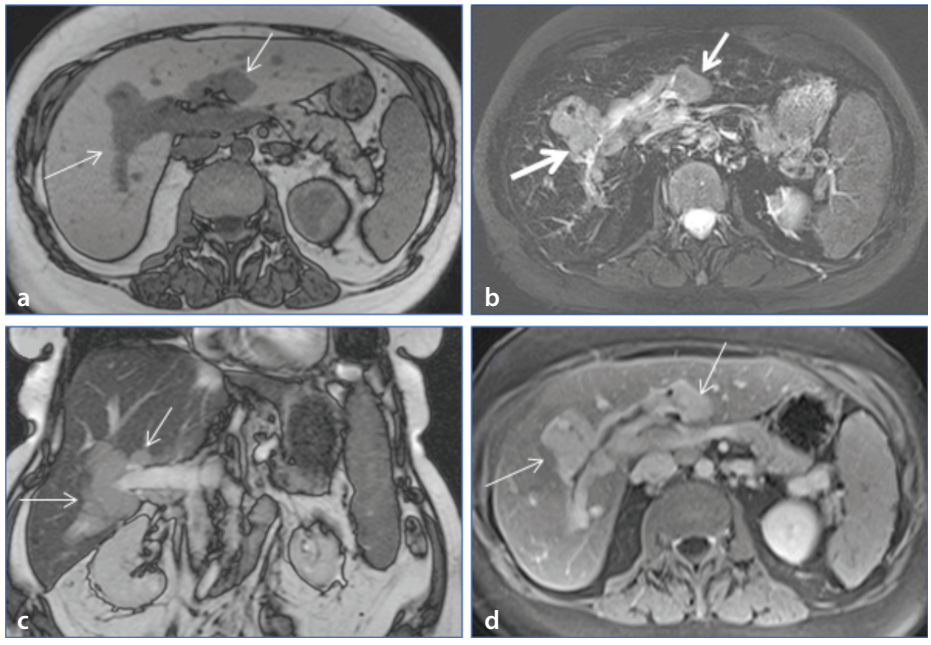

Figure 6. Axial T1-weighted image **(a)**, axial T2-weighted image with fat suppression **(b)**, coronal T2-weighted image **(c)**, and axial T1-weighted image with fat suppression in the late arterial phase **(d)** in a 56-year-old woman with extramedullary hematopoiesis and myelofibrosis showing periportal masses (white arrows), demonstrating low signal intensity on the T1-weighted images, high signal intensity in the T2-weighted images, and progressive enhancement after contrast administration.

organ transplant recipients, the second most common site in patients with AIDS, and the least common site in patients with congenital immunodeficiencies.[21,25-31]

The imaging characteristics of EBV-associated smooth muscle tumors are generally non-specific. On CT, the tumors present as hypodense lesions, often with rim enhancement[22,32] and sometimes with central necrosis.[21,27] Findings on MRI typically include isointensity on T1-weighted images and isointensity to mild hyperintensity on T2-weighted images, with substantial contrast enhancement (Figure 7).[33] Diagnosis is confirmed through immunohistochemistry, which shows positivity for smooth muscle actin and EBV-encoded RNA.[22]

Differentiating EBV-associated smooth muscle tumors from non-EBV-related primary or metastatic smooth muscle tumors of the liver, such as leiomyosarcomas, is crucial because of the latter's less favorable prognosis. Even without intervention, EBV-associated tumors tend to progress slowly.[17,22]

Hepatobiliary tuberculosis and tuberculomas

Hepatobiliary tuberculosis and tuberculomas of the liver most commonly occur in patients with disseminated disease. In an autopsy series, a hepatosplenic prevalence of 80% to 100% was seen in the setting of pulmonary miliary disease.[34,35] There are three types of hepatobiliary tuberculosis: parenchymal (including the miliary, nodular, and mixed subtypes), biliary, and serohepatic.[36] Imaging plays a key role in the diagnosis and management of these patients because the symptoms of patients with these lesions are often vague and non-specific, potentially delaying appropriate treatment. Most cases ultimately require tissue sampling to confirm the diagnosis.

In parenchymal hepatobiliary tuberculosis, imaging findings typically identify multiple (<2 cm) well-defined nodules throughout the liver that may contain calcifications (Figure 8). Larger lesions (>2 cm) in the less commonly seen macronodular type of hepatobiliary tuberculosis tend to demonstrate peripheral rim enhancement and central necrosis on CT, and they may contain chunky peripheral or central calcifications (Figure 9).[37] However, their appearance is dependent on the degree of caseous necrosis and liquefaction. On CT imaging, non-caseating granulomas appear hypoattenuating with no or mild peripheral rim enhancement.[38] However, lesions with caseous necrosis and liquefaction can resemble pyogenic abscesses with a honeycomb appearance, multiple enhancing septations, and regions of scattered necrosis.[38] On MRI , macronodular lesions typically appear as T1 hypointense. On T2-weighted images, they have varied intensity (hypointense to hyperintense) with peripheral T2-hypointense rims, and on postcontrast sequences, they have heterogenous enhancement.[36,39] Larger macronodular nodules may represent the fusion of miliary and/or micronodular nodules. Mixed parenchymal lesions have imaging findings of both the miliary and nodular types. Sonographically, these lesions usually appear uniformly hypoechoic or heterogeneous, with intermixed echogenic and hypoechoic regions.[40] However, lesions with other patterns have been observed, including -rarely- hypoechoic to echogenic lesions with echogenic centers.[40] The lesion borders tend to be poorly defined, but this too varies. The imaging characteristics of these lesions can be non-specific and can vary depending on the stage of the hepatic granuloma. Therefore, tissue sampling is often required to confirm the diagnosis.

Tuberculous cholangitis is a rare pre-

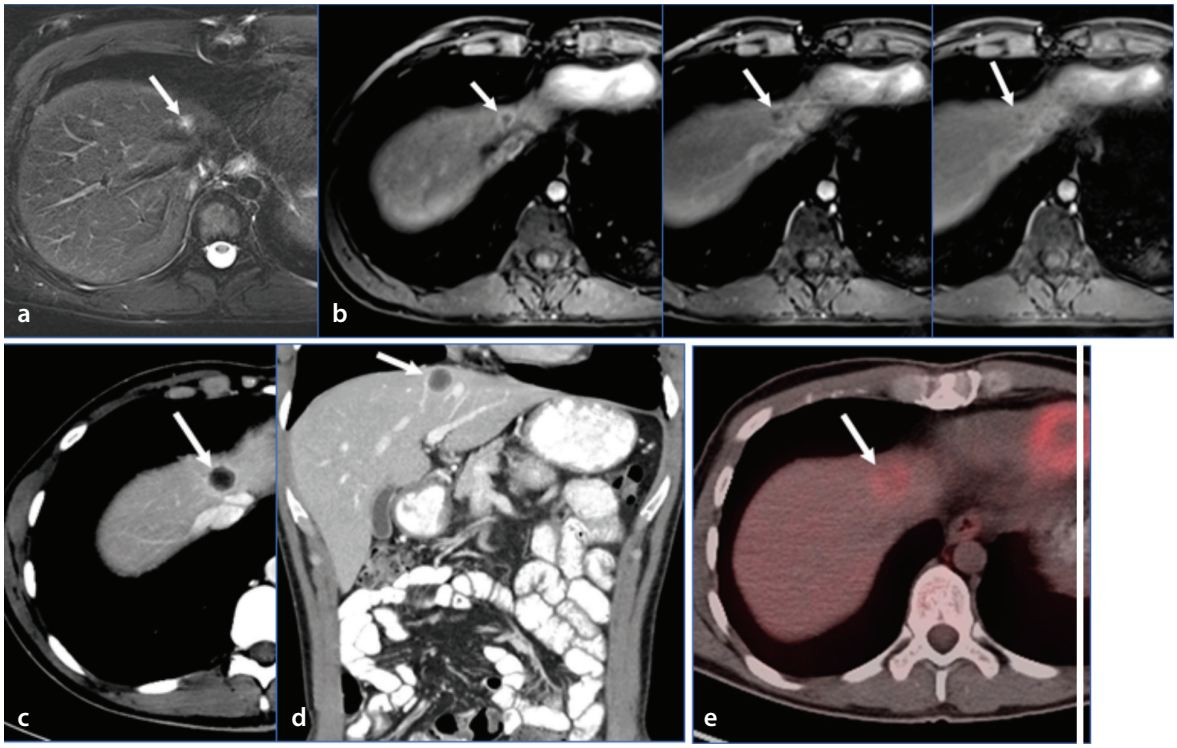

Figure 7. Images from a 26-year-old woman with stage IVb monomorphic posttransplant lymphoproliferative disorder involving the bones and lymph nodes. The patient presented with a slowly growing liver mass identified as an Epstein–Barr virus-associated smooth muscle tumor. Axial T2-weighted images **(a)** and three dynamic gadolinium-enhanced T1-weighted images with fat suppression **(b)** showing a small T2-hyperintense lesion in the left hepatic lobe (arrows). The lesion exhibits early peripheral enhancement and some delayed fill-in of contrast material with persistent peripheral enhancement. Axial **(c)** and coronal **(d)** contrast-enhanced computed tomography images obtained 15 months later showing a mild increase in lesion size (arrows). Peripheral enhancement was observed, and the center of the lesion had an attenuation of approximately 15 HU. An axial positron emission tomography/computed tomography scan **(e)** showing the lesion's increased metabolic activity (standardized uptake value: 3.87). HU, Hounsfield units

Figure 8. Transabdominal ultrasound scan **(a)** showing a heterogeneously echogenic lesion (arrow) with a peripheral rim of increased echogenicity. Axial unenhanced computed tomography images **(b, c)** showing multiple calcified lesions (arrows). Some of the lesions have a target-like appearance, with central and peripheral calcifications separated by a zone of soft-tissue attenuation. This was a biopsy-verified tuberculoma.

sentation of hepatobiliary tuberculosis and primarily occurs in children.[38] Imaging findings consist of dilated irregular intrahepatic ducts or diffuse miliary calcifications along the affected bile ducts.[41] Involvement of the biliary tree may be caused by biliary tract contamination from enteric mycobacterium infection, hematogenous spread, or direct extension from adjacent infected structures (e.g., caseating granuloma or hilar lymphadenopathy).[40]

The serohepatic type of hepatobiliary tuberculosis is the rarest form. Imaging findings consist of multiple hypoattenuating nodules in a subcapsular distribution with a thickened hepatic capsule.[36] These findings give the liver a characteristic appearance of subcapsular nodularity, which has been characterized as having "sugar coating" or a "frosted liver" appearance.[41]

The diagnosis of serohepatic hepatobiliary tuberculosis should be considered among high-risk patients or in those who have suspected tuberculous involvement of the lungs, spleen, or lymph nodes. A defini-

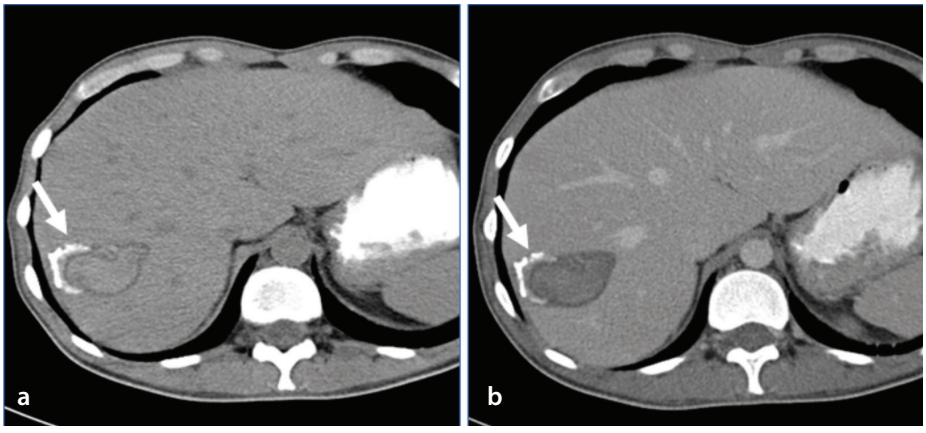

Figure 9. Biopsy-verified tuberculoma with a history of AIDS and disseminated tuberculosis. Axial unenhanced **(a)** and contrast-enhanced **(b)** computed tomography images demonstrating a lesion in the right hepatic lobe (arrows). The unenhanced image shows central high attenuation, a peripheral rim of low attenuation, and an incomplete ring of calcification. No enhancement was identified after contrast administration.

tive diagnosis is made with acid-fast staining and with histology revealing caseating granulomas.[42]

Peliosis hepatis

Peliosis hepatitis is an uncommon lesion characterized by abnormal sinusoidal dilatation and multiple blood-filled lacunar spaces.[43] It is thought to be caused by hepatic flow obstruction at the sinusoidal level and is potentially caused by steroids, oral contraceptives, cytotoxic drugs, chronic lung disease, infections (e.g., HIV and tuberculosis), and various malignancies (especially hepatomas).[44] In HIV-related peliosis hepatis, *Bartonella henselae* has been identified as a causative agent, with regression after appropriate antibiotic therapy.[45] Peliosis hepatitis can also develop in patients with a renal or cardiac transplant. Hematologic disorders, diabetes, and necrotizing vasculitis also seem to be associated with peliosis hepatis. However, up to 50% of peliosis hepatis cases are idiopathic.[44] These lesions are normally asymptomatic, but they may cause symptoms if they rupture and hemorrhage. Additional complications include portal hypertension, cholestasis, liver enlargement, ascites, and even liver failure.

Two different pathologic forms of peliosis hepatitis have been described: the phlebectatic and parenchymal types. The phlebectatic type is characterized by blood-filled cavities lined with endothelial cells and an aneurysmal dilatation of the central vein. By contrast, in the parenchymal type, the blood-filled cavities are not lined by endothelial cells, and it occurs in the setting of hemorrhagic parenchymal necrosis.[46,47]

Lesions typically measure up to a few centimeters and usually demonstrate no mass effect on transiting vessels. Imaging features vary according to the age of the blood components and the presence or absence of hepatic steatosis. On ultrasound, these lesions tend to be hypoechoic in the setting of background steatosis and hyperechoic in the setting of normal liver tissue with increased perinodular or intranodular vascular flow on Doppler imaging.

On multiphasic CT and MRI, peliosis hepatitis lesions exhibit intralesional hemorrhage and predominantly progressive centrifugal enhancement, although centripetal enhancement is also possible (Figure 10). The appearance of these lesions can vary based on the age of the hemorrhagic components.[48] Cavities within these lesions that communicate with sinusoids demonstrate enhancement in line with that of blood vessels, whereas thrombosed portions are not enhanced. These lesions usually demonstrate early discontinuous (globular) arterial enhancement. In atypical cases where the enhancement is centripetal rather than classic centrifugal, the lesions may be mistaken for hemangiomas.[48]

Sarcoidosis

Sarcoidosis is a multisystemic inflammatory disease that is histologically defined by the formation of non-necrotic granulomas. The cause of sarcoidosis remains unclear, but currently accepted theories suggest that a genetic predisposition and exposure to environmental or occupational antigens lead to a dysfunctional immune response.[49] The disease mainly affects young and middle-aged adults, and there is a slight predominance in women compared with men.[49] Although all populations worldwide are affected, some studies report increased rates among African Americans and people from the Nordic countries.[50]

The lungs are the most common site of involvement; however, every organ system can be affected. Hepatic disease is reported in up to 80% of cases.[50,51] The formation of hepatic granulomas can incite an inflammatory response leading to fibrosis and, eventually, cirrhosis.[50] Most patients with hepatic sarcoidosis (50%–80%) are asymptomatic. Symptoms include fatigue, fever, weight loss, pruritus, jaundice, and abdominal pain.[50]

Imaging findings in sarcoid-related liver disease are often non-specific and vary substantially. In most patients with sarcoidosis, the liver appears normal on imaging. The most common finding, reported in up to 29% of cases, is hepatomegaly.[51,52] Other abnormalities include portal hypertension, portal vein or hepatic vein thrombosis, and cirrhosis.[51,53]

Focal hepatic lesions are also a feature in a small percentage of patients with sarcoidosis. They often appear as multiple small lesions, which can coalesce and form larger lesions.[51,52] On non-contrast CT, these lesions are usually hypodense (Figure 11), whereas on MRI , the lesions are typically T1 isointense or slightly hypointense and T2 hypointense. However, increases in lesion size, the coalescence of larger granulomas, or active inflammation can result in hyperintense T2-weighted signal intensity.[54] On both imaging modalities, lesions are hypoenhancing relative to the surrounding parenchyma (Figure 12). Concomitant lesions can also be seen within the spleen, and portal lymphadenopathy may also be present. Both of these findings can aid in diagnosis.[55]

Cholestasis is another feature of hepatic sarcoidosis, and it can result in intrahepatic or extrahepatic biliary ductal dilatation.[52,53] The latter could also be secondary to disease involving the common hepatic duct or extrinsic compression from enlarged lymph nodes. The appearance may mimic that of a primary biliary tumor, necessitating caution during imaging interpretation.[52]

Amyloidosis

Amyloidosis is a general term referring to a group of disorders characterized by the deposition of misfolded serum proteins -amyloid fibrils- in extracellular spaces.[56] Amyloid

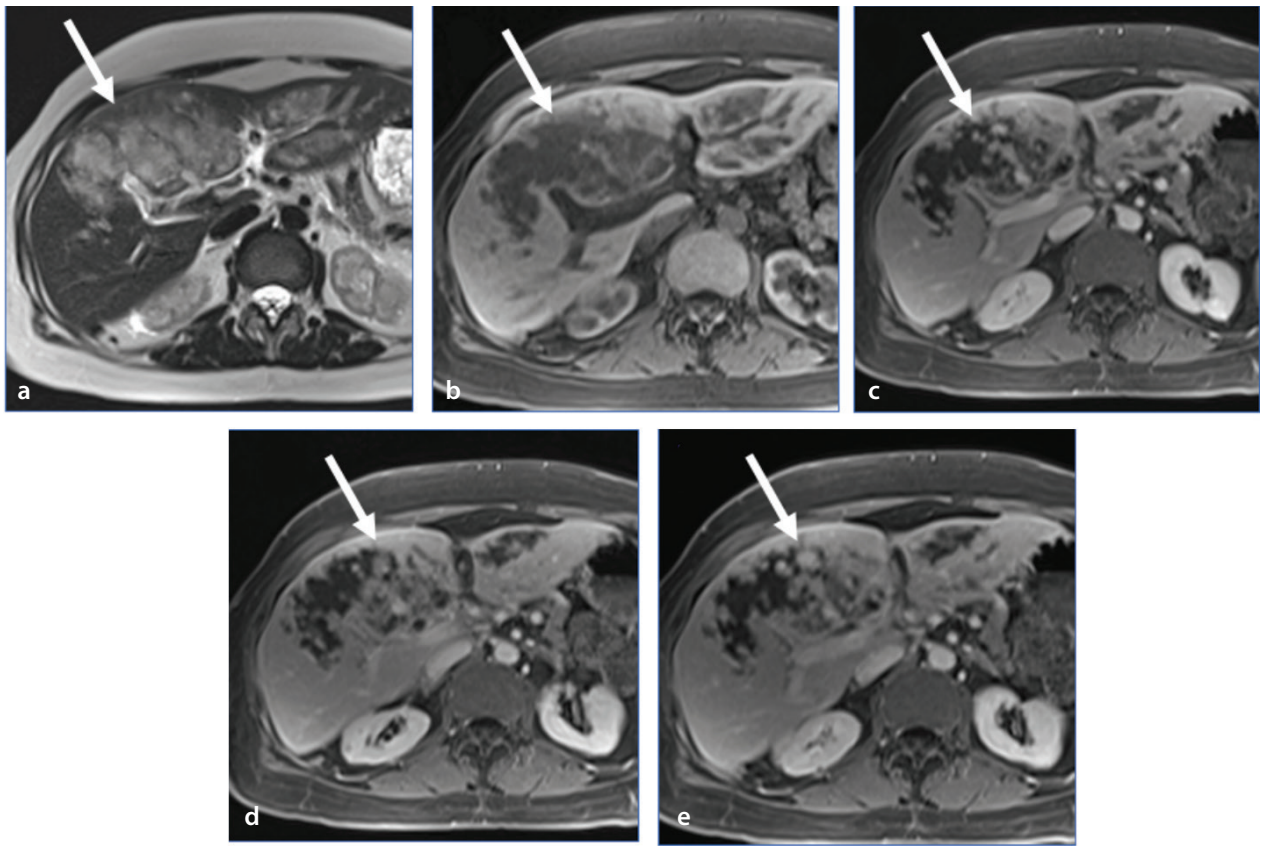

Figure 10. Axial T2-weighted images **(a)** and dynamic post-gadolinium T1-weighted images with fat suppression **(b-e)** showing a large hepatic mass (long arrows) spanning both lobes of the liver and demonstrating high T2 signal intensity, low T1 signal intensity, and progressive centripetal enhancement following contrast administration. The lesion represents a biopsy-verified peliosis hepatis that was not present 3 years earlier. Despite its large size, no appreciable mass effect was identified. Vessels are observed coursing through the lesion without significant attenuation.

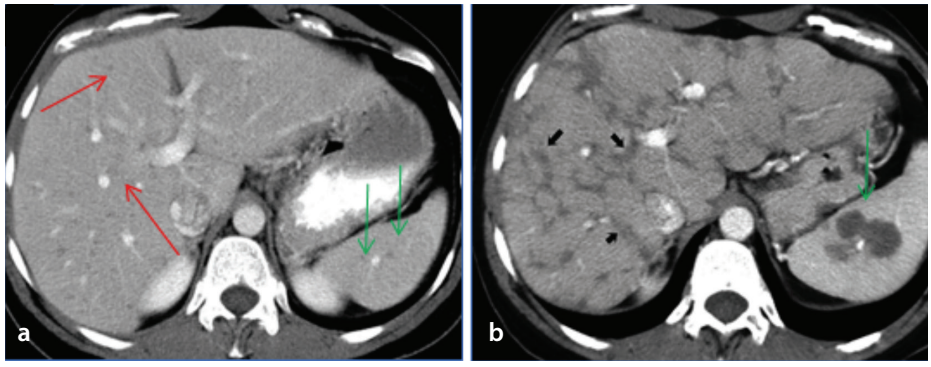

Figure 11. Contrast-enhanced computed tomography (CECT) images from a patient with a long history of pulmonary sarcoidosis. **(a)** Initial CECT image showing multiple subtle hypodense hepatic (red arrows) and splenic (green arrows) lesions. CECT image from the same patient obtained 5 years after the initial scan **(b)** showing extensive periportal and bridging non-enhancing fibrous septa throughout the liver (black arrows) with periportal predominance. Note the interval increase in the multiple hypoattenuating splenic lesions (green arrow).

fibrils result when precursor proteins that are usually soluble aggregate, forming insoluble fibers that are resistant to degradation.[56-58] In localized amyloidosis, the formation and deposition of amyloid fibrils occurs in the same organ. In systemic amyloidosis, the formation of the amyloid fibrils occurs in one organ, and the deposition of the fibrils occurs in a distant location.[58] Systemic amyloidosis can be classified into multiple types, depending on the precursor protein; over 15 types of precursor proteins have been described.[58] Common conditions associated with the systemic form of the disease include plasma cell disorders, malignancy, and chronic infection or inflammation.[56-58]

Amyloidosis can affect all organ systems. In the abdomen, amyloid deposition occurs in the genitourinary and gastrointestinal tracts as well as in the liver, spleen, peritoneum, and retroperitoneum.[56]

Within the liver, amyloid fibril deposition occurs in the perisinusoidal spaces and along the blood vessel walls.[59,60] As with sarcoidosis, imaging findings in the liver can be non-specific, and amyloidosis most commonly manifests as hepatomegaly.[61] Some reported patterns that can mimic other infiltrative liver diseases, such as steatosis and hepatic venous congestion, include diffusely decreased attenuation on CT, heterogeneity of liver parenchyma, and heterogeneous contrast enhancement.[59,61] More well-defined masses, along with focal and diffuse calcifications, can also occur (Figure 13).[61]

On MRI, diffusely decreased signal intensity on T2-weighted images has been observed, possibly from amyloid deposition and/or increased iron deposition in the liver occurring secondary to amyloid-associated chronic renal disease.[60,61] Increased liver stiffness has also been observed and can be evaluated using magnetic resonance elastography.[59,62]

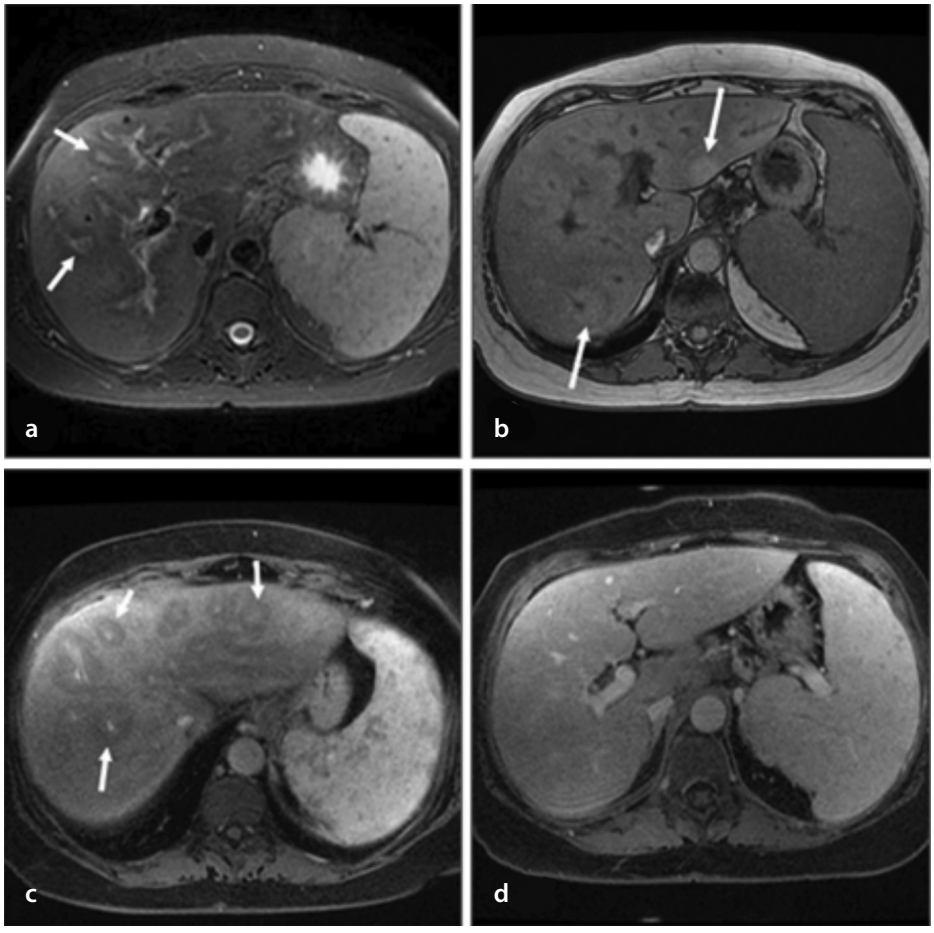

Figure 12. Axial T2-weighted image with fat suppression **(a)**, axial T1-weighted opposed-phase image **(b)**, axial T1-weighted late-arterial-phase image with fat suppression **(c)**, and axial T1-weighted portal-venous-phase image with fat suppression (d) in a patient with sarcoidosis showing periportal masses (white arrows), demonstrating slightly increased signal intensity and poor enhancement during the late arterial phase. The areas of abnormal signaling were not identified during the portal venous phase. There is also evidence of splenic involvement with splenomegaly and multiple small granulomas.

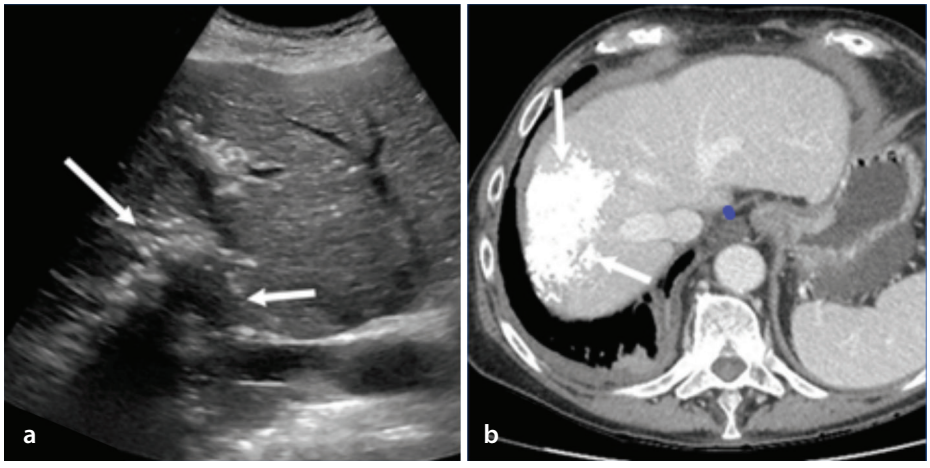

Figure 13. Transabdominal ultrasound scan **(a)** showing an echogenic mass-like structure (white arrows) with posterior shadowing caused by calcifications. Contrast-enhanced computed tomography scan **(b)** showing a mass-like structure (white arrows) within the right hepatic lobe related to extensive calcifications. The patient was diagnosed with hepatic amyloidosis.

In conclusion, a large variety of pathologies can present within the liver, and this can make diagnosing liver lesions challenging. Although most lesions are common tumors, on rare occasions, radiologists may encounter one of the aforementioned rare lesions. By being familiar with these lesions and including them in the differential diagnosis, radiologists and clinicians can ensure that patients receive the correct diagnosis and treatment.

Conflict of interest disclosure

The authors declared no conflicts of interest.

References

1. Stringer MD, Alizai NK. Mesenchymal hamartoma of the liver: a systematic review. *J Pediatr Surg*. 2005;40(11):1681-1690. [CrossRef]
2. Assarzadegan N, Montgomery E. Uncommon benign neoplasms and pseudotumors of the liver. *Arch Pathol Lab Med*. 2023;147(4):390-402. [CrossRef]
3. Kim SH, Kim WS, Cheon JE, et al. Radiological spectrum of hepatic mesenchymal hamartoma in children. *Korean J Radiol*. 2007;8(6):498-505. [CrossRef]
4. Papke DJ Jr. Mesenchymal neoplasms of the liver. *Surg Pathol Clin*. 2023;16(3):609-634. [CrossRef]
5. Wang D, Misdraji J. Inflammatory pseudotumor of the liver. *Surg Pathol Clin*. 2023;16(3):565-580. [CrossRef]
6. Kim KA, Kim KW, Park SH, et al. Unusual mesenchymal liver tumors in adults: radiologic-pathologic correlation. *AJR Am J Roentgenol. 2006;*187(5):481-489. [CrossRef]
7. Roberts AS, Shetty AS, Mellnick VM, Pickhardt PJ, Bhalla S, Menias CO. Extramedullary haematopoiesis: radiological imaging features. *Clin Radiol*. 2016;71(9):807-814. [CrossRef]
8. Sohawon D, Lau KK, Lau T, Bowden DK. Extramedullary haematopoiesis: a pictorial review of its typical and atypical locations. *J Med Imaging Radiat Oncol*. 2012;56(5):538-544. [CrossRef]
9. La Fianza A, van der Byl G, Maccabelli G, Torretta L, Calliada F. CT and MR findings in extramedullary haematopoiesis with biliary system encasement: a case report. *J Radiol Case Rep*. 2010;4(11):1-8. [CrossRef]
10. Jelali MA, Luciani A, Kobeiter H, et al. MRI features of intrahepatic extramedullary haematopoiesis in sickle cell anaemia. *Cancer Imaging*. 2006;6(1):182-185. [CrossRef]
11. Navarro M, Crespo C, Pérez L, Martínez C, Galant J, González I. Massive intrahepatic extramedullary hematopoiesis in myelofibrosis. *Abdom Imaging*. 2000;25(2):184-186. [CrossRef]

12. Malla S, Razik A, Das CJ, Naranje P, Kandasamy D, Kumar R. Marrow outside marrow: imaging of extramedullary haematopoiesis. *Clin Radiol*. 2020;75(8):565-578. [CrossRef]
13. Kwak HS, Lee JM. CT findings of extramedullary hematopoiesis in the thorax, liver and kidneys, in a patient with idiopathic myelofibrosis. *J Korean Med Sci*. 2000;15(4):460-462. [CrossRef]
14. Gupta P, Naran A, Auh YH, Chung JS. Focal intrahepatic extramedullary hematopoiesis presenting as fatty lesions. *AJR Am J Roentgenol*. 2004;182:1031-1032. [CrossRef]
15. Wong Y, Chen F, Tai KS, et al. Imaging features of focal intrahepatic extramedullary haematopoiesis. *Br J Radiol*. 1999;72(861):906-910. [CrossRef]
16. Kapatia G, Kaur A, Rastogi P, et al. Extramedullary hematopoiesis: clinical and cytological features. *Diagn Cytopathol*. 2020;48(3):191-196. [CrossRef]
17. Dekate J, Chetty R. Epstein-Barr virus-associated smooth muscle tumor. *Arch Pathol Lab Med*. 2016;140(7):718-722. [CrossRef]
18. Pritzker KP, Huang SN, Marshall KG. Malignant tumours following immunosuppressive therapy. *Can Med Assoc J*. 1970;103(13):1362-1365. [CrossRef]
19. Chadwick EG, Connor EJ, Hanson IC, et al. Tumors of smooth-muscle origin in HIV-infected children. *JAMA*. 1990;263(23):3182-3184. [CrossRef]
20. Lee ES, Locker J, Nalesnik M, et al. The association of Epstein-Barr virus with smooth-muscle tumors occurring after organ transplantation. *N Engl J Med*. 1995;332(1):19-25. [CrossRef]
21. Hussein K, Rath B, Ludewig B, Kreipe H, Jonigk D. Clinico-pathological characteristics of different types of immunodeficiency-associated smooth muscle tumours. *Eur J Cancer*. 2014;50(14):2417-2424. [CrossRef]
22. Gallien S, Zuber B, Polivka M, et al. Multifocal Epstein-Barr virus-associated smooth muscle tumor in adults with AIDS: case report and review of the literature. *Oncology*. 2008;74(3-4):167-176. [CrossRef]
23. Deyrup AT, Lee VK, Hill CE, et al. Epstein-Barr virus-associated smooth muscle tumors are distinctive mesenchymal tumors reflecting multiple infection events: a clinicopathologic and molecular analysis of 29 tumors from 19 patients. *Am J Surg Pathol*. 2006;30(1):75-82. [CrossRef]
24. McClain KL, Leach CT, Jenson HB, et al. Association of Epstein-Barr virus with leiomyosarcomas in children with AIDS. *N Engl J Med*. 1995;332(1):12-18. [CrossRef]
25. Jenson HB, Leach CT, McClain KL, et al. Benign and malignant smooth muscle tumors containing Epstein-Barr virus in children with AIDS. *Leuk Lymphoma*. 1997;27:303-314. [CrossRef]
26. Suankratay C, Shuangshoti S, Mutirangura A, et al. Epstein-Barr virus infection-associated smooth-muscle tumors in patients with AIDS. *Clin Infect Dis*. 2005;40(10):1521-1528. [CrossRef]
27. Jossen J, Chu J, Hotchkiss H, et al. Epstein-Barr virus-associated smooth muscle tumors in children following solid organ transplantation: a review. *Pediatr Transplant*. 2015;19(2):235-243. [CrossRef]
28. Yu L, Aldave AJ, Glasgow BJ. Epstein-Barr virus-associated smooth muscle tumor of the iris in a patient with transplant: a case report and review of the literature. *Arch Pathol Lab Med*. 2009;133(8):1238-1241. [CrossRef]
29. Reyes C, Abuzaitoun O, De Jong A, Hanson C, Langston C. Epstein-Barr virus-associated smooth muscle tumors in ataxia-telangiectasia: a case report and review. *Hum Pathol*. 2002;33(1):133-136. [CrossRef]
30. Shaw RK, Issekutz AC, Fraser R, et al. Bilateral adrenal EBV-associated smooth muscle tumors in a child with a natural killer cell deficiency. *Blood*. 2012;119(17):4009-4012. [CrossRef]
31. Tulbah A, Al-Dayel F, Fawaz I, Rosai J. Epstein-Barr virus-associated leiomyosarcoma of the thyroid in a child with congenital immunodeficiency: a case report. *Am J Surg Pathol*. 1999;23(4):473-476. [CrossRef]
32. Conrad A, Brunet AS, Hervieu V, et al. Epstein-Barr virus-associated smooth muscle tumors in a composite tissue allograft and a pediatric liver transplant recipient. *Transpl Infect Dis*. 2013;15(5):182-186. [CrossRef]
33. Lohan R, Bathla G, Gupta S, Hegde AN. Epstein-Barr virus (EBV)-related smooth muscle tumors of central nervous system--a report of two cases and review of literature. *Clin Imaging*. 2013;37(3):564-568. [CrossRef]
34. Kumar V, Pandey D. Isolated hepatosplenic tuberculosis. *Hepatobiliary Pancreat Dis Int*. 2008;7(3):328-330. [CrossRef]
35. Thoeni RF, Margulis AR. Gastrointestinal tuberculosis. *Semin Roentgenol*. 1979;14(4):283-294. [CrossRef]
36. Yu RS, Zhang SZ, Wu JJ, Li RF. Imaging diagnosis of 12 patients with hepatic tuberculosis. *World J Gastroenterol*. 2004;10(11):1639-1642. [CrossRef]
37. Leder RA, Low VH. Tuberculosis of the abdomen. *Radiol Clin North Am*. 1995;33(4):691-705. [CrossRef]
38. Joshi AR, Basantani AS, Patel TC. Role of CT and MRI in abdominal tuberculosis. *Curr Radiol Rep*. 2014;2:66. [CrossRef]
39. Levine C. Primary macronodular hepatic tuberculosis: US and CT appearances. *Gastrointest Radiol*. 1990;15:307-309. [CrossRef]
40. Chong VH, Lim KS. Hepatobiliary tuberculosis. *Singapore Med J*. 2010;51(9):744-751. [CrossRef]
41. Kakkar C, Polnaya AM, Koteshwara P, Smiti S, Rajagopal KV, Arora A. Hepatic tuberculosis: a multimodality imaging review. *Insights Imaging*. 2015;6(6):647-658. [CrossRef]
42. Karaosmanoglu AD, Onur MR, Sahani DV, Tabari A, Karcaaltincaba M. Hepatobiliary tuberculosis: imaging findings. AJR A*m J Roentgenol*. 2016;207(4):694-704. [CrossRef]
43. Zak FG. Peliosis hepatis. *Am J Pathol*. 1950;26(1):1-15. [CrossRef]
44. Wanless IR. Vascular disorders. In: MacSweenRNM, Burt AD, Portmann BC, Ishak KG, Scheuer PJ, Anthony PP, eds. Pathology of the Liver, 4th ed. Glasgow, UK: Churchill Living-stone; 2002:553-555. [CrossRef]
45. Koehler JE. Bartonella-associated infections in HIV-infected patients. AIDS *Clin Care*. 1995;(12):97-102. PMID: 11362939. [CrossRef]
46. Vignaux O, Legmann P, de Pinieux G, et al. Hemorrhagic necrosis due to peliosis hepatis: imaging findings and pathological correlation. *Eur Radiol*. 1999;9(3):454-456. [CrossRef]
47. Yanoff M, Rawson AJ. Peliosis hepatis. An anatomic study with demonstration of two varieties. *Arch Pathol*. 1964;77:159-165. [CrossRef]
48. Iannaccone R, Federle MP, Brancatelli G, et al. Peliosis hepatis: spectrum of imaging findings. *AJR Am J Roentgenol*. 2006;187(1):43-52. [CrossRef]
49. Drent M, Crouser ED, Grunewald J. Challenges of sarcoidosis and its management. *N Engl J Med*. 2021;385(11):1018-1032. [CrossRef]
50. Moser A, Cheung A. Hepatic sarcoidosis: a review of the diagnosis and management. *Curr Hepatol Rep*. 2024;23(9):137-144. [CrossRef]
51. Karaosmanoğlu AD, Onur MR, Saini S, Taberi A, Karcaaltincaba M. Imaging of hepatobiliary involvement in sarcoidosis. Abdom Imaging. *Abdom Imaging*. 2015;40(8):3330-3337. [CrossRef]
52. Warshauer DM, Lee JK. Imaging manifestations of abdominal sarcoidosis. *AJR Am J Roentgenol*. 2004;182(1):15-28. [CrossRef]
53. Ferreira A, Ramalho M, de Campos RO, et al. Hepatic sarcoidosis: MR appearances in patients with chronic liver disease. *Magn Reson Imaging*. 2013;31(3):432-438. [CrossRef]
54. Jung G, Brill N, Poll LW, Koch JA, Wettstein M. MRI of hepatic sarcoidosis: large confluent lesions mimicking malignancy. *AJR Am J Roentgenol*. 2004;183(1):171-173. [CrossRef]
55. Koyama T, Ueda H, Togashi K, Umeoka S, Kataoka M, Nagai S. Radiologic manifestations of sarcoidosis in various organs. *Radiographics*. 2004;24(1):87-104. [CrossRef]
56. Krauß LU, Schmid S, Mester P, et al. Clinical, Endoscopic, and histopathologic observations in gastrointestinal amyloidosis. *J Gastrointestin Liver Dis*. 2023;32(4):497-506. [CrossRef]

57. Rambaran RN, Serpell LC. Amyloid fibrils: abnormal protein assembly. *Prion*. 2008;2(3):112-117.

58. Muchtar E, Dispenzieri A, Magen H, et al. Systemic amyloidosis from A (AA) to T (ATTR): a review (Review). *J Intern Med.* 2021;289(3):268-292. [CrossRef]

59. Özcan HN, Haliloğlu M, Sökmensüer C, Akata D, Özmen M, Karçaaltıncaba M. Imaging for abdominal involvement in amyloidosis. *Diagn Interv Radiol.* 2017;23(4):282-285. [CrossRef]

60. Venkatesh SK, Hoodeshenas S, Venkatesh SH, et al. Magnetic resonance elastography of liver in light chain amyloidosis. *J Clin Med.* 2019;8(5):739. [CrossRef]

61. Kim SH, Han JK, Lee KH, et al. Abdominal amyloidosis: spectrum of radiological findings. *Clin Radiol*. 2003;58(8):610-620. [CrossRef]

62. Sugi MD, Kawashima A, Salomao MA, Bhalla S, Venkatesh SK, Pickhardt PJ. Amyloidosis: multisystem spectrum of disease with pathologic correlation. *Radiographics*. 2021;41(5):1454-1474. [CrossRef]